frontiers | Frontiers in Physiology

TYPE Original Research
PUBLISHED 14 August 2024
DOI 10.3389/fphys.2024.1440720

OPEN ACCESS

EDITED BY
Ian Michael Thornell,
The University of Iowa, United States

REVIEWED BY
Mark Oliver Bevensee,
University of Alabama at Birmingham, United States
Kirk L. Hamilton,
University of Otago, New Zealand
Gergely Gyimesi,
University of Bern, Switzerland

*CORRESPONDENCE
Mark D. Parker,
parker28@buffalo.edu

RECEIVED 29 May 2024
ACCEPTED 30 July 2024
PUBLISHED 14 August 2024

CITATION
Pasternack RA, Quade BN, Marshall A and Parker MD (2024) NH_3/NH_4^+ allosterically activates SLC4A11 by causing an acidic shift in the intracellular pK that governs $H^+(OH^-)$ conductance.
Front. Physiol. 15:1440720.
doi: 10.3389/fphys.2024.1440720

NH_3/NH_4^+ allosterically activates SLC4A11 by causing an acidic shift in the intracellular pK that governs $H^+(OH^-)$ conductance

Richard A. Pasternack[1], Bianca N. Quade[1], Aniko Marshall[1] and Mark D. Parker[1,2]*

[1]Department of Physiology and Biophysics, The State University of New York: The University at Buffalo, Buffalo, NY, United States, [2]Department of Ophthalmology, The State University of New York: The University at Buffalo, Buffalo, NY, United States

SLC4A11 is the most abundant membrane transport protein in corneal endothelial cells. Its functional presence is necessary to support the endothelial fluid pump that draws fluid from the corneal stroma, preventing corneal edema. Several molecular actions have been proposed for SLC4A11 including H_2O transport and cell adhesion. One of the most reproduced actions that SLC4A11 mediates is a H^+ (or OH^-) conductance that is enhanced in the presence of NH_4Cl. The mechanism by which this occurs is controversial with some providing evidence in favor of NH_3-H^+ cotransport and others providing evidence for uncoupled H^+ transport that is indirectly stimulated by the effects of NH_4Cl upon intracellular pH and membrane potential. In the present study we provide new evidence and revisit previous studies, to support a model in which NH_4Cl causes direct allosteric activation of SLC4A11 by means of an acidic shift in the intracellular pK (pK_i) that governs the relationship between intracellular pH (pH_i) and SLC4A11 H^+-conductance. These findings have important implications for the assignment of a physiological role for SLC4A11.

KEYWORDS

acid-base, Btr1, NaBC1, cornea, proton

1 Introduction

The members of the SLC4 family of solute carrier proteins are mainly Na^+-independent and Na^+-dependent Cl^-/HCO_3^- exchangers or Na^+-coupled HCO_3^- (or $CO_3^=$) transporters (Parker and Boron, 2013; Lee et al., 2022). SLC4A11 (originally named "BTR1": Bicarbonate Transporter Related Protein 1) was the last member of the SLC4 family to be cloned (Parker et al., 2001) and is the only member of the family that does not transport $HCO_3^-/CO_3^=$ (Jalimarada et al., 2013; Ogando et al., 2013; Loganathan et al., 2016). Instead, SLC4A11 influences intracellular pH (pH_i) by conducting H^+, or its thermodynamic equivalent OH^- (Kao et al., 2015; Myers et al., 2016). For convenience hereafter, and in the absence of any definitive data in favor of one substrate over the other, we will assume that H^+ are the transported species. SLC4A11 is expressed at low levels in many tissues, but appears to have most functional impact in the cornea and inner ear as evidenced by the corneal dystrophies and progressive hearing loss that are caused by SLC4A11 mutations in both humans and mice (Vithana et al., 2006; 2008; Desir et al., 2007; Lopez et al., 2009; Gröger et al., 2010; Han et al., 2013).

Most studies of SLC4A11 have focused on its role in the cornea. Here, SLC4A11 is expressed in the basolateral membrane of the corneal endothelial cells that line the posterior (aqueous-humor facing side) of the cornea (Vilas et al., 2013). These cells are responsible for pumping fluid from the corneal stroma to prevent it from swelling and losing its ability to optimally transmit and refract light (Hodson, 1977). SLC4A11 is clearly valuable for endothelial pumping because autosomal recessive inheritance of SLC4A11 mutations cause congenital hereditary endothelial dystrophy (CHED), a non-progressive corneal thickening and opacification (Vithana et al., 2006). Furthermore, an apparently discrete set of SLC4A11 mutations result in autosomal dominant inheritance of a late-onset form of Fuchs endothelial corneal dystrophy (FECD4), which typically manifests from the 4th decade of life, preceded by the appearance of excrescences from the Descemet's membrane that underlie the endothelial cells, which are known as guttae (Weiss et al., 2024). However, the mechanism by which SLC4A11 loss compromises the endothelial pump remains elusive because there is little consensus about SLC4A11's molecular action.

The earliest proposal for SLC4A11 action was that it, like plantal Slc4-like proteins, performed borate transport: specifically electrogenic $2Na^+$-$B(OH)_4^-$ cotransport (Frommer and von Wirén, 2002; Park et al., 2004). This hypothesis fell out of favor due to an inability of others to find evidence for this mode of action with mammalian SLC4A11 (Jalimarada et al., 2013; Ogando et al., 2013; Vilas et al., 2013; Kao et al., 2015; Loganathan et al., 2016). That original characterization study also attributed an EIPA-insensitive Na^+/H^+ exchanger-like activity to SLC4A11, but neither the EIPA-sensitivity nor the Na^+-dependence of this H^+ transport activity has proven to be universally repeatable, leaving open the possibility that such results were influenced by endogenous activities (Park et al., 2004; Ogando et al., 2013; Kao et al., 2015; 2016; Zhang et al., 2015; Myers et al., 2016). Other reported SLC4A11 transport modes include a H_2O permeability that is disturbed by disease-causing mutations (Vilas et al., 2013), a role in extracellular matrix adhesion (Malhotra et al., 2020), and a conditional presence in mitochondria (Ogando et al., 2019). Any of these, alone or in combination, remain a feasible explanation for loss of endothelial pump function with SLC4A11 mutation. However, at present, none of these features has been investigated by more than one group.

In this study, we focus on the robust and repeatable Na^+-independent H^+ transport action of SLC4A11, an action that is stimulated by increases in pH_i, extracellular pH (pH_e), and NH_4Cl (Zhang et al., 2015; Myers et al., 2016; Kao et al., 2020; Quade et al., 2020) and which is also disrupted by disease-causing mutations (Kao et al., 2015; Quade et al., 2022). However, there remains a controversy over whether the NH_4Cl-stimulated action of SLC4A11 represents SLC4A11-mediated NH_3-H^+ cotransport (Zhang et al., 2015; Kao et al., 2020) or an indirect stimulation of SLC4A11-mediated H^+ conductance caused by cellular depolarization and sub-membranous alkalinization of pH_i due to NH_3 movement across the lipid bilayer (Myers et al., 2016). A recent attempt to distinguish NH_3-H^+ cotransport from NH_4^+ or H^+ transport using the Goldman-Hodgkin-Katz approach led to the conclusion that SLC4A11 operates in competing modes of NH_3-H^+ cotransport or unaccompanied H^+ transport, with the inference that the presence of NH_3/NH_4^+ inhibits unaccompanied H^+ conduction (Kao et al., 2020). These are important distinctions as they inform the predicted direction of transport, the interpretation of SLC4A11 structure, and the ultimately the physiological role of SLC4A11. In our previous work, we demonstrated that SLC4A11-mediated H^+ transport is governed by an intracellular pK (pK_i), the value of which can be modulated by changes in pH_e and by disease-causing mutations (Quade et al., 2020; Quade et al., 2022). At pH_e = 7.50, pK_i is too alkaline to be determined, but can be no more acidic than 7.6 (Quade et al., 2020). However, when we raise pH_e, pK_i is shifted into measurable range. For example, pK_i for human SLC4A11 ~ 7.04 when pH_e = 8.50 (Quade et al., 2022). This acidic-shift in pK_i manifests as a rise in SLC4A11 current. We note that no study of SLC4A11 activity has directly measured transmembrane NH_3/NH_4^+ movement, relying instead on proxies such as pH and voltage changes. With that as context, here we revisit the phenomenon of NH_4Cl-stimulation of SLC4A11-mediated H^+ currents to determine whether it could be explained by a direct allosteric effect of NH_3/NH_4^+ upon SLC4A11 pK_i.

2 Results

2.1 Determining pK_i for SLC4A11 at pH_e = 8.50

In a previous study we determined that pK_i for human SLC4A11 at pH_e = 8.50 is 7.04 ± 0.01 (Quade et al., 2022). For this study we generated a contemporary set of control data to confirm the pK_i of human SLC4A11 at pH_e = 8.50 in new experimental hands. As we have previously reported, SLC4A11-expressing oocytes slowly alkalinize upon exposure to pH_e = 8.50 solution, and the rate of alkalinization can be enhanced by clamping the membrane potential (V_m) at a value more positive than the predicted reversal potential for H^+ (E_H). An example of this phenomenon can see seen in the first figure of Quade et al. (2022). As pH_i rises, we gather a series of I-V plots such that each I-V plot can be assigned to a value of pH_i. Figure 1A shows a selection of these plots gathered from a single SLC4A11-expressing oocyte as pH_i is caused to rise under voltage-clamp. Note that the slope of the I-V relationship (i.e., membrane conductance, G_m) rises as pH_i increases. The relationship between pH_i and G_m is shown for six SLC4A11-expressing cells in Figure 1B, in which the trace marked by black diamonds is the full data set from the cell shown in Figure 1A. The average $G_{m.max}$ was 90 ± 14 μS. Also shown in Figure 1B are resting pH_i/G_m relationships from six H_2O-injected cells (crosses) for which the average G_m was 2 ± 1 μS. In order to extract pK_i values from the SLC4A11 data, we first normalize G_m data from each cell to its own $G_{m,max}$ (Figure 1C) and fit those data to the Hill equation, generating the best-fit relationships described by a pK_i and an apparent Hill coefficient (N_{app}) shown as gray lines in Figure 1D. The average of these relationships is represented as a black dotted-line in Figure 1. We calculate an average pK_i of 7.08 ± 0.04 for human SLC4A11 at pH_e = 8.50, which is not different from the range

10.3389/fphys.2024.1440720

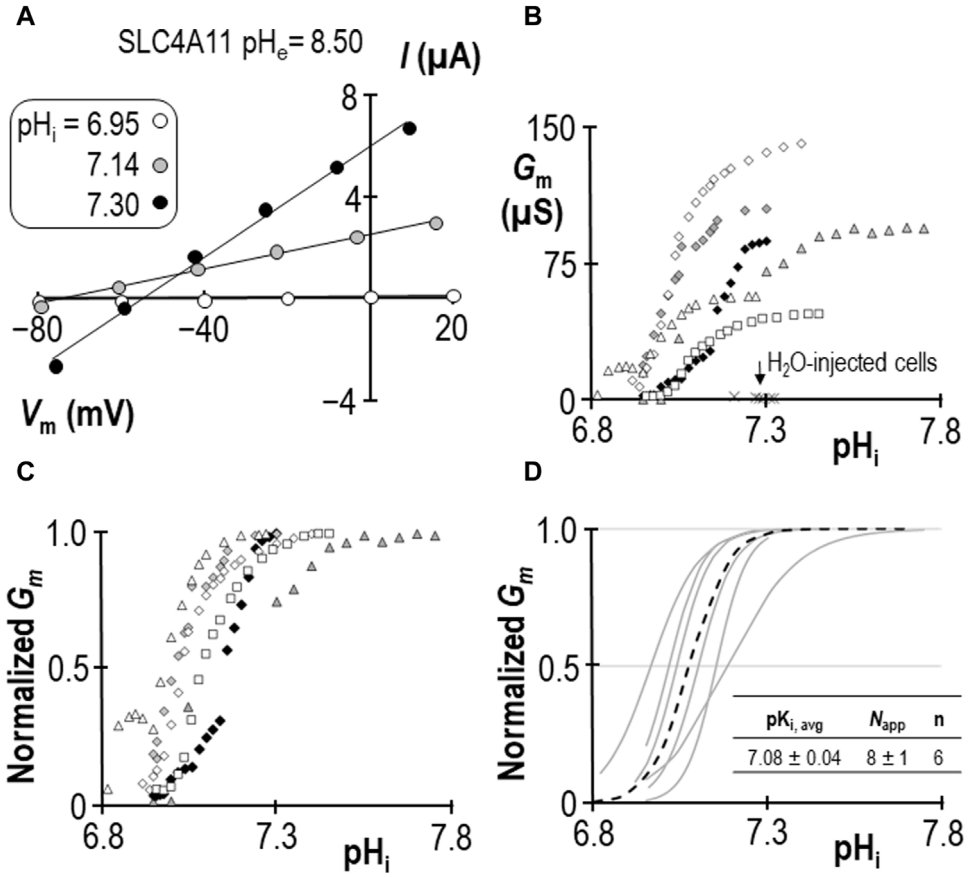

FIGURE 1
SLC4A11 behavior in the absence of NH_4Cl (extracellular pH = 8.50) **(A)** A representative selection of current-voltage (I-V) relationships gathered from a single SLC4A11-expressing oocyte as intracellular pH (pH_i) rises. **(B)** The relationship between pH_i and slope conductance (G_m) from the full-set of I-V relationships gathered from the SLC4A11-expressing cell shown in panel (A) (black diamonds) and from five other SLC4A11-expressing cells (each represented by its own symbol). The pH_i versus G_m relationship at resting pH_i for five H_2O-injected oocytes is represented by crosses. **(C)** SLC4A11 data from panel (B), normalized to its respective maximum G_m ($G_{m,max}$). **(D)** Best-fit lines for each cell to the Hill equation are shown in gray. The dashed black line represents the Hill equation generated using the average pK_i and apparent Hill coefficients (N_{app}) of the n = 6 replicates, as shown in the inset table.

that we had previously determined in Quade et al. (2022) (p = 0.32, two-tailed, unpaired t-test).

2.2 Determining pK_i for SLC4A11 at pH_e = 8.50 in the presence of 1 mM NH_4Cl

The response of SLC4A11-expressing oocytes in pH_e = 8.50 solution was altered in two ways in the presence of 1 mM NH_4Cl. First, as shown in the example in Figure 2A, the cell acidified rather than alkalinized (initial $dpH_i/dt = 5.1 \pm 0.9 \times 10^{-4}$ pH units/s, n = 6). This was also a feature of H_2O-injected cells (initial $dpH_i/dt = 5.5 \pm 0.8 \times 10^{-4}$ pH units/s, n = 6, Figure 2A inset). Second, unique to SLC4A11-expressing cells, G_m unexpectedly rose to a plateau (over period "a") and subsequently declined to a value close to its starting value (over period "b") when pH_i was further acidified by clamping V_m at a value more negative than E_H. Let us first focus our attention on period "b," during which acidification causes a familiar decline. Figure 2B shows a selection of responses from the cell represented in Figure 2A. The pH_i versus G_m relationships gathered from seven SLC4A11-expressing cells during period "b" are plotted in Figure 2C. The average $G_{m,max}$ was 89 ± 5 μS, which is not different from that for the group of cells assayed in the absence of NH_4Cl (p = 0.94, two-tailed unpaired t-test). Also shown in Figure 2C are resting pH_i/G_m relationships from six control cells (originally injected with H_2O in place of SLC4A11 cRNA) that were acidified prior to assay by HCl injection (crosses). The average G_m of these cells was 11 ± 2 μS. Best-fit normalized G_m versus pH_i data for SLC4A11-expressing cells is shown in Figure 2D. We calculate that the average pK_i for SLC4A11-expressing cells at pH_e = 8.50 in the presence of 1 mM NH_4Cl is 6.28 ± 0.05, which is significantly more acidic than the pK_i range determined in the absence of NH_4Cl (p < 0.001, one-tailed, unpaired t-test). On the other hand, there was no significant difference in the value of N_{app} compared to its value in the absence of NH_4Cl (P = 0.17, two-tailed unpaired t-test).

Does the action of SLC4A11 during period "a" represent a second pK_i that reports acid-activation? We hypothesized that period "a" represented the time during which pK_i was transitioning between its ± NH_4Cl values. If we assume that neither $G_{m,max}$ nor N_{app} change in a single SLC4A11-expressing oocyte during the course of

10.3389/fphys.2024.1440720

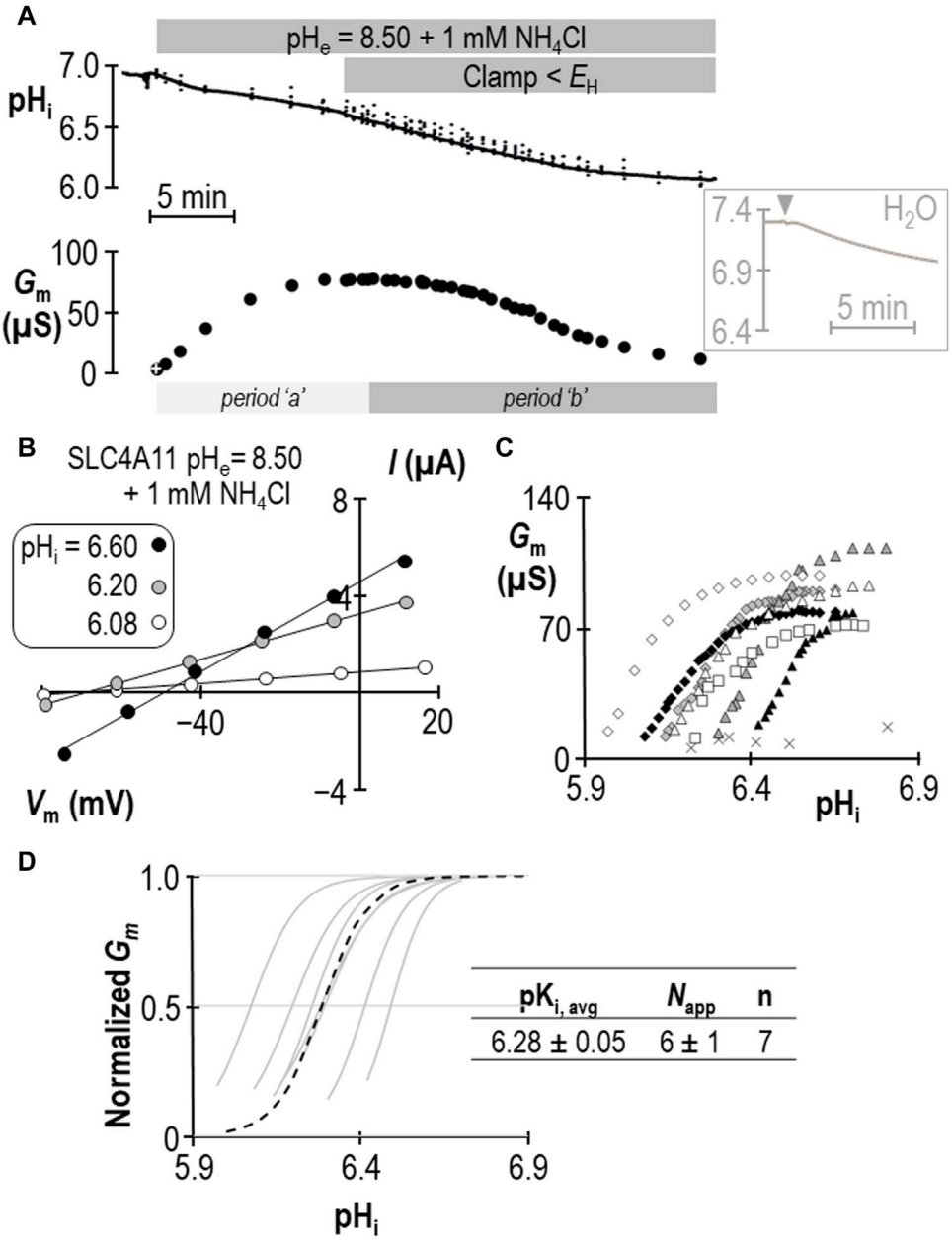

FIGURE 2
SLC4A11 behavior in the presence of 1 mM NH_4Cl (extracellular pH = 8.50). **(A)** A representative example of the pH_i (top) and G_m (bottom) response of an SLC4A11-expressing oocyte to the addition of 1 mM NH_4Cl. The first G_m point in the data series (white cross) was gathered prior to the presence of NH_4Cl. The inset shows a representative pH_i response to the addition of 1 mM NH_4Cl (point of solution change indicated by gray triangle) of a H_2O-injected cell at pH_e = 8.50. **(B)** A representative selection of I-V relationships gathered from a single SLC4A11-expressing oocyte as pH_i falls during period "b". **(C)** The relationship between pH_i and G_m from the full-set of I-V relationships gathered from the SLC4A11-expressing cell shown in panel (B) (black diamonds) and from six other SLC4A11-expressing cells (each represented by its own symbol). The pH_i versus G_m relationship for six H_2O-injected oocytes after acidification by HCl injection is represented by crosses. **(D)** Best-fit lines for each cell to the Hill equation are shown in gray. The dashed black line represents the Hill equation generated using the average pK_i and N_{app} of the n = 7 replicates, as shown in the inset table.

an experiment such as that in Figure 2A, we can solve the Hill equation to generate an apparent pK_i ($pK_{i,app}$) for each point in the experiment at which we have paired values of G_m and pH_i. The results of this approach are shown in Figure 3A and support the hypothesis that period "a" is dynamic time of pK_i adjustment, while period "b" represents a time over which SLC4A11 has assumed a new and relatively stable pK_i. In three of our seven experiments, we extended the protocol to examine a period "c" (example shown in Figure 3B) during which we could examine the behavior of SLC4A11 in the pH-range of period "a", but after SLC4A11 has assumed its + NH_4Cl pK_i. As shown in Figure 3C, SLC4A11 exhibits a similar pK_i during period "b" versus period "c" pK_i (P = 0.19: two-tailed, paired t-test) and does not revisit the apparent acid-activated behavior exhibited during period "a." In summary for this section, we find that the presence of 1 mM NH_4Cl results in a significant acidic shift in the value of pK_i for human SLC4A11 at pH_e = 8.50.

10.3389/fphys.2024.1440720

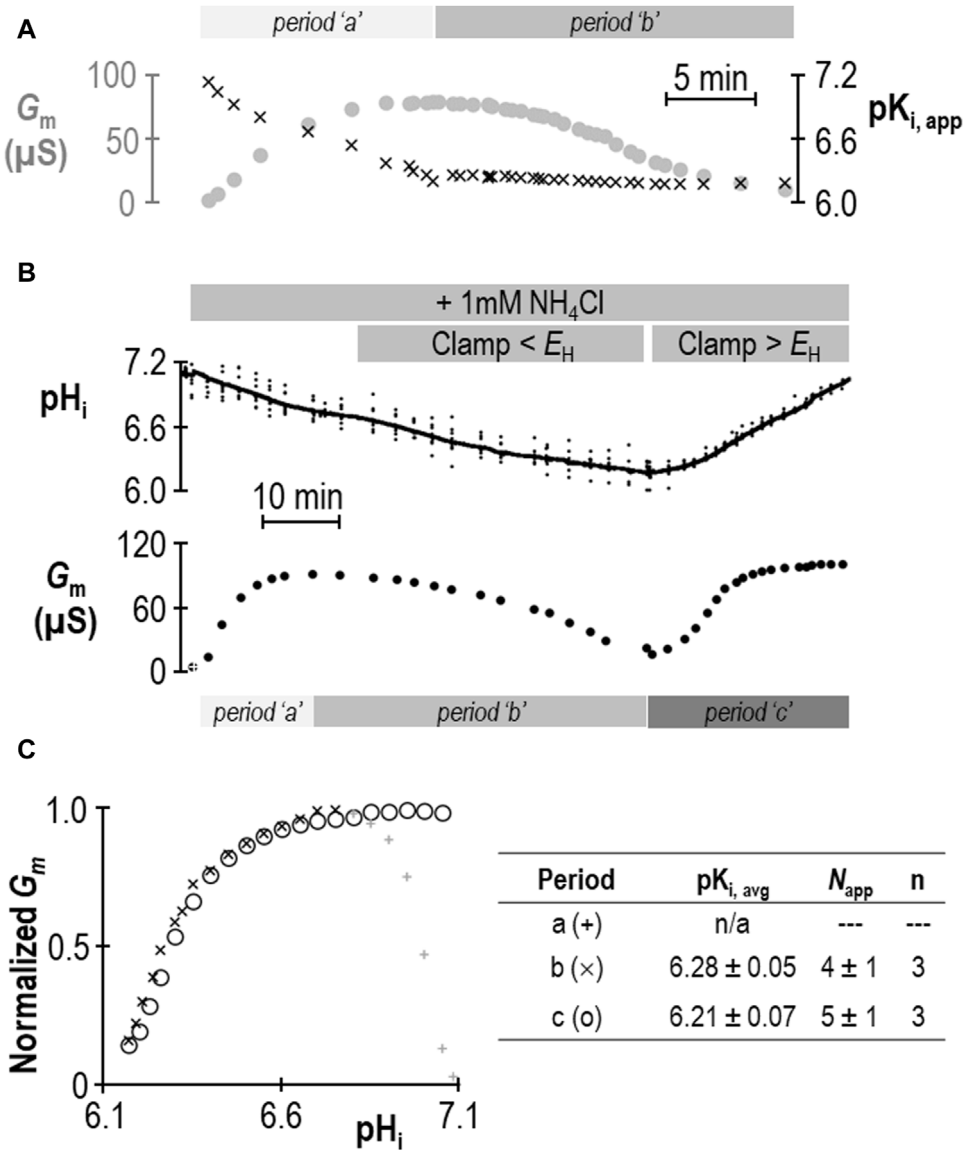

Period	$pK_{i, avg}$	N_{app}	n
a (+)	n/a	---	---
b (×)	6.28 ± 0.05	4 ± 1	3
c (o)	6.21 ± 0.07	5 ± 1	3

FIGURE 3
Validation of change in SLC4A11 pK_i upon addition of NH_4Cl. **(A)** G_m data from Figure 2A replotted with the apparent pK_i ($pK_{i,app}$) calculated from the pH_i at each value of G_m. **(B)** A representative experiment similar to that shown in Figure 2A, extended into a third experimental period in which G_m is monitored during a return to starting pH_i. **(C)** G_m values from panel (B) plotted for each of the three experimental periods, normalized to $G_{m,max}$ for each period. The inset table shows pK_i and N_{app} for periods "b" and "c" calculated from best-fit data to the Hill equation for three such experiments.

2.3 Determining the ion-selectivity of SLC4A11 in the presence of 1 mM NH_4Cl

In an earlier study we demonstrated that for SLC4A11-expressing oocytes, the relationship between V_m and the transmembrane pH gradient (64 mV/pH-unit) was close to Nernstian with respect to H^+ (Myers et al., 2016). Figure 4A shows equivalent data gathered in the presence of 1 mM NH_4Cl from experiments such as those shown in Figures 2A, 3B. The average slope of the relationship is 71 ± 5 mV/decade (Figure 4B) with an *x*-axis intercept of −1.25 ± 0.04 (Figure 4C). Data from one of the three Figure 3B-style experiments is highlighted in Figure 4A, with black data points taken from period "b" and white data points taken from period "c." In summary for this section, the slope of the relationship between V_m and transmembrane pH gradient does not appear to be greatly disturbed by the presence of 1 mM NH_4Cl, except for the unusual observation that the relationship does not intersect with the origin. The meaning of this observation is explored in Section 3.3.

2.4 Comparing the influence of pH_e and [NH_3] on SLC4A11 pK_i

Using a similar work-flow to that described above, we determined the pK_i of SLC4A11 at pH_e = 7.50 in the presence of 1 mM NH_4Cl (Figures 5A–C). $G_{m.max}$ in this cohort of cells was 104 ± 7 μS, which is not different from the equivalent range reported

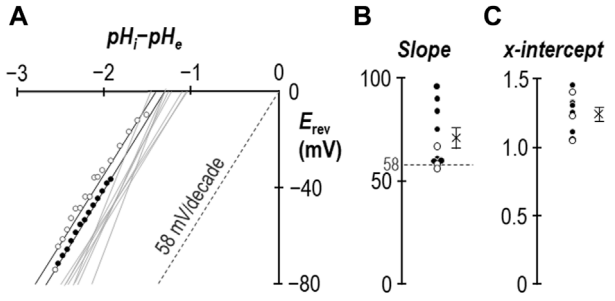

FIGURE 4
The ion-selectivity of SLC4A11 in the presence of NH_4Cl. **(A)** The relationship between V_m and the transmembrane pH gradient (pH_i-pH_e), determined from the experiments represented in Figures 2, 3, are shown by solid gray lines. One example data set is shown in full from period "b" (filled circles) and period "c" (open circles). The Nernstian slope of ideal H^+ selectivity is shown as a gray dashed line. **(B)** The average slopes calculated from the data in panel (A) are shown as filled (data gathered during period "b") and open (data gathered during period "c") circles. The cross represents the average of these data. **(C)** The average x-intercepts calculated from the data in panel (A) are shown as filled (data gathered during period "b") and open (data gathered during period "c") circles. The cross represents the average of these data.

from cells assayed at pH_e = 8.50 + NH_4Cl (p = 0.09: two-tailed, unpaired t-test). Because the ratio of NH_3:NH_4^+ is pH-sensitive, we also determined the pK_i of SLC4A11 at pH_e = 8.50 in the presence of 0.12 mM NH_4Cl (Figures 6A–C). In both conditions, although [NH_4Cl] is different, [NH_3] is the same (0.017 mM) Figure 6D summarizes the values of pK_i that have been determined during this study. We find that pKi at pHe = 7.50 in the presence of 1 mM NH_4Cl is 7.06 ± 0.05 (Figure 5C), and the pK_i at pH_e = 8.50 in the presence of 0.12 mM NH_4Cl is 7.04 ± 0.05 (Figure 6C). These values are not significant different from each other (p = 0.68: two-tailed, unpaired t-test).

We can make two additional statistical comparisons: [1] at pH_e = 8.50, pK_i is not significantly different in the presence or absence of 0.12 mM NH_4Cl (P = 0.50: two-tailed, unpaired t-test), and [2] in the presence of 1 mM NH_4Cl, raising pH_e from 7.50 to 8.50 has a significant acidifying effect on pK_i (p< 0.01: two-tailed, unpaired t-test). The interpretation of these findings are discussed in Section 3.4.

3 Discussion

3.1 NH_4Cl increases SLC4A11 G_m by shifting pK_i in the acidic direction

Our data show that, at pH_e = 8.50, the extracellular presence of 1 mM NH_4Cl results in a significant acidic shift in pK_i such that, at almost any value of pH_i between 6.0 and 7.3 (i.e., the range bounded by the two ± NH_4Cl traces: solid and dashed black-lines in Figure 7A), G_m would be increased. A formal determination of pK_i at physiological pH_e in the absence of NH_4Cl has been precluded by a practical limitation on how high we can raise oocyte pH_i, but we have previously estimated that the value must be more alkaline than 7.6 (Quade et al., 2020). The ability of NH_4Cl to cause an acidic shift in pK_i, enables us to determine a pK_i range of 7.06 ± 0.05 at pH_e = 7.50 in the present study. Thus, we can imagine that, even with the conservative estimate of the NH_4Cl-free pK_i, the implication is similar: the presence of NH_4Cl would cause an increase in G_m at typical physiological values of pH_i (e.g., 7.0–7.3, which is included in the range bounded by the solid and dashed gray-lines in Figure 7A). Critically, this stimulatory effect of NH_4Cl represents only an increase in G_m caused by a redefinition of the pH_i versus G_m relationship. Neither $G_{m,max}$ nor N_{app} are significantly altered by NH_4Cl (at least as determined at pH_e = 8.50) so the redefinition appears to represent a direct acidic-translation of the relationship. Although we are wary of assigning any meaning to the numerical value of N_{app} (which is a function of the number of titratable moieties within SLC4A11), the observation of an unchanging N_{app} at least implies that mechanism by which SLC4A11 responds to pH_i is similarly complex in the absence and presence of NH_4Cl.

We had once before investigated the role of NH_4Cl in stimulating SLC4A11 (Myers et al., 2016). We found, as others had before us (Zhang et al., 2015), that the presence of 5 mM NH_4Cl causes an increase in SLC4A11 G_m (or I_m at fixed V_m in the case of those other studies). However, although we appreciated at that time that SLC4A11 was pH_i-dependent, we did not consider the possibility that the relationship between pH_i and G_m could be modulated. The addition of 5 mM NH_4Cl to (even H_2O-injected) oocytes causes a rapid and robust depolarization (Musa-Aziz et al., 2009). This action in itself is sufficient to drive SLC4A11-mediated H^+ efflux, resulting in a cellular alkalinization that further activates SLC4A11 (Myers et al., 2016). Thus, in that study, when we increased G_m to $G_{m.max}$ at pH_e = 8.50 by adding 5 mM NH_4Cl and saw no change in that value upon NH_4Cl removal (maintaining a voltage clamp at 0 mV to mimic the depolarizing effect of NH_4Cl presence), we assumed that the presence of NH_4Cl was merely causing G_m to rise according to the prescribed pH_i vs. G_m relationship. In light of our new data, we reinterpret those data as likely to have been gathered at a pH_i value that was greater than the NH_4Cl-free pK_i, where G_m values for both ± NH_4Cl relationships are close to $G_{m,max}$. That is to say that we reinterpret our data in favor of a model in which NH_4Cl causes a direct rather than indirect allosteric activation of SLC4A11.

3.2 Data do not conclusively support a more important role for NH_3 versus NH_4^+ for SLC4A11 action

Models in which SLC4A11 transports NH_3/NH_4^+ favor a NH_3:nH^+ cotransport mechanism over NH_4^+ transport because NH_3 increases in concentration with rising pH, thereby providing an explanation for the greater stimulation of SLC4A11 currents/conductance at pH_e = 8.50 than pH_e = 7.50. We might use the same logic to conclude that NH_3 is more likely than NH_4^+ to be the allosterically activating species. However, our data provide an alternative explanation: as shown in Figures 7A,B, at the typical resting pH_i range for SLC4A11-expressing oocytes [6.9–7.0: (Quade et al., 2020)], the shift in pK_i makes less difference to G_m at pH_e =

10.3389/fphys.2024.1440720

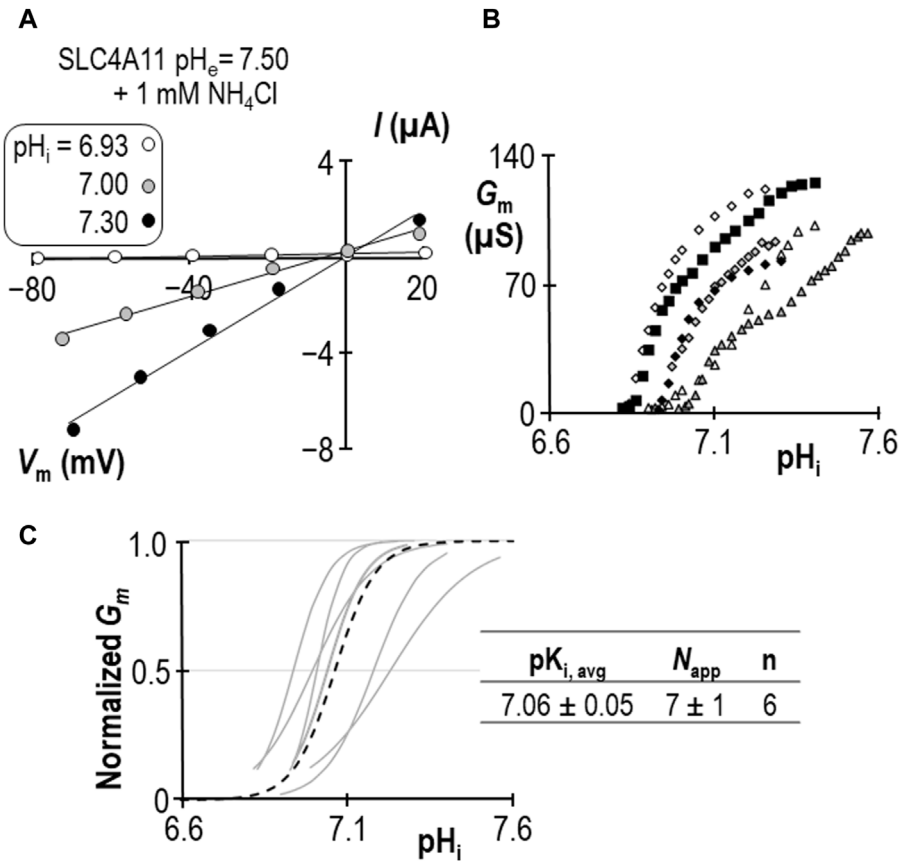

FIGURE 5
SLC4A11 behavior in the presence of 1 mM NH_4Cl (extracellular pH = 7.50). **(A)** A representative selection of current-voltage (I-V) relationships gathered from a single SLC4A11-expressing oocyte as intracellular pH (pH_i) rises. **(B)** The relationship between pH_i and slope conductance (G_m) from the full-set of I-V relationships gathered from the SLC4A11-expressing cell shown in panel (A) (black diamonds) and from five other SLC4A11-expressing cells (each represented by its own symbol). **(C)** Best-fit lines for each cell to the Hill equation are shown in gray. The dashed black line represents the Hill equation generated using the average pK_i and apparent Hill coefficients (N_{app}) of the n = 6 replicates, as shown in the inset table.

7.50 (light gray arrow in Figures 7A,B/upper panel) than at pH_e = 8.50 (dark gray arrow in Figures 7A,B/lower panel). In this case it is not necessary to invoke a model in which the abundance of the substrate/activator is pH dependent; NH_4^+ (whose fractional abundance is relatively unchanged between pH_e 7.50 and 8.50) could be considered equally likely to be the species responsible for the observed stimulation.

Our data do not speak definitively to the nature of the activating species. We believe, because the time course of pK_i shift (>10 min: Figure 3A) is much slower than the rate of solution turnover in the bath (<1 min) that the allosteric activation likely requires the activating species to accumulate intracellularly in order to exert its effect on SLC4A11. Because the handling of NH_3/NH_4^+ by oocytes is unusually complex (Musa-Aziz et al., 2009), it is difficult to specifically relate this time course of activation to the accumulation of either species. On the one hand NH_3 is presumed to be the more membrane permeable of the two species. On the other hand, in contrast to the expected alkalinization observed in mammalian cells exposed to NH_4Cl, (even H_2O-injected) oocyte pH_i paradoxically acidifies as if NH_4^+ is accumulating faster, perhaps entering via non-selective cation channels as NH_3 is sequestered in sub-membranous granules (Burckhardt and Frömter, 1992). For this reason, it is not clear whether there is a diagnostically useful differential in their rate of accumulation that could point to one species over the other.

3.3 SLC4A11 retains H^+ selectivity in the presence of NH_4Cl

Another critical parameter that is unchanged in the presence of NH_4Cl is its H^+ selectivity, because the V_m of SLC4A11-expressing cells exhibits a close-to-Nernstian response to changes in the transmembrane pH gradient (Figure 4). This suggests that SLC4A11 remains a selective H^+ conductor rather than assuming a novel NH_3-coupling mode. Although previous studies have claimed to provide evidence of NH_3-coupled H^+ transport using a similar approach (Zhang et al., 2015; Kao et al., 2020), we believe that these finding should be interpreted with caution as the approach violates necessary assumptions of reversal potential calculations: chiefly that substrates can only cross the membrane via SLC4A11 (not true for NH_3) and that V_m is dominated by the action of SLC4A11 (not true due to the depolarizing action of NH_3/NH_4^+). In the absence of a specific inhibitor for SLC4A11, to distinguish the

10.3389/fphys.2024.1440720

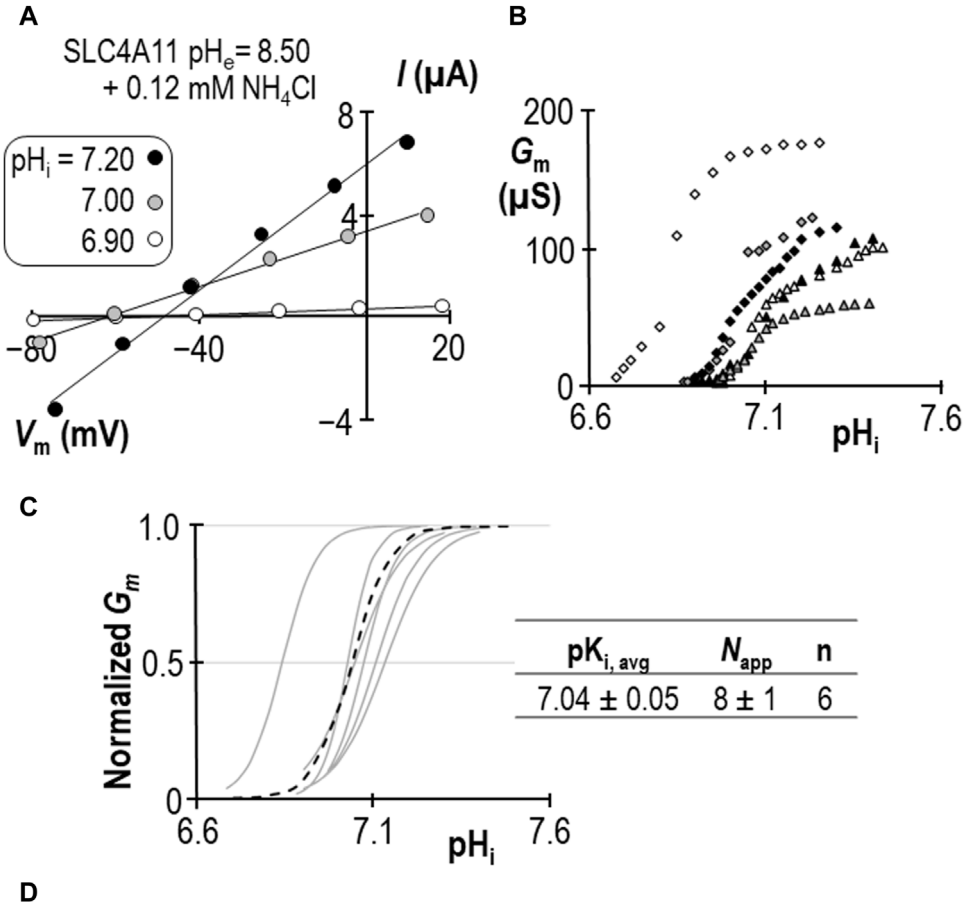

D

	[NH_3]: 0 mM	0.017 mM	0.151 mM
pH_e =7.50	>7.6 (Quade et al., 2020)	7.06 ± 0.05 (1mM NH_4Cl)	--- (8.64mM NH_4Cl)
pH_e=8.50	7.08 ± 0.04	7.04 ± 0.05 (0.12 mM NH_4Cl)	6.28 ± 0.05 (1mM NH_4Cl)

FIGURE 6
SLC4A11 behavior in the presence of 0.12 mM NH_4Cl (extracellular pH = 8.50). **(A)** A representative selection of current-voltage (I-V) relationships gathered from a single SLC4A11-expressing oocyte as intracellular pH (pH_i) rises. **(B)** The relationship between pH_i and slope conductance (G_m) from the full-set of I-V relationships gathered from the SLC4A11-expressing cell shown in panel (A) (black diamonds) and from five other SLC4A11-expressing cells (each represented by its own symbol). **(C)** Best-fit lines for each cell to the Hill equation are shown in gray. The dashed black line represents the Hill equation generated using the average pK_i and apparent Hill coefficients (N_{app}) of the n = 6 replicates, as shown in the inset table. **(D)** A summary of the pK_i of SLC4A11 detemined under the various conditions tested in this study.

behavior of the protein from that of the system, the best that such calculations may achieve is a description of the permeability of the system (i.e., SLC4A11 and its membrane environment). One such study concluded that SLC4A11 was capable of both NH_3:H^+ cotransport and H^+ transport (Kao et al., 2020). If so, this is not the typical action of an obligatorily coupled cotransport protein and could equally describe the behavior of a H^+ conductor in an NH_3-permeable membrane.

There is one unusual aspect to our reversal potential data that requires further explanation. In previous studies we have found that the relationship between the transmembrane gradient and V_m for wild-type SLC4A11 crosses the *x*-axis at a value close to zero as expected for a H^+ conductor. In the present study performed in the presence of NH_4Cl, we find that the relationship is substantially offset from the origin and intersects the *x*-axis at −1.25 pH-units as if we had underestimated pH_i by 1.25 units. This is not impossible, as seven of the ten data sets were gathered while SLC4A11 was mediating H^+ influx and thus pH immediately below the membrane may have been more acidic than bulk pH_i being measured at the tip of our microelectrode, which is impaled deeper into the cell. However, three of these data sets were gathered while SLC4A11 was mediating H^+ efflux, and exhibited the same offset, so we do not believe that this can be the correct explanation. An alternate explanation is illustrated in Figure 8. Here we show that, if we consider these data as being

10.3389/fphys.2024.1440720

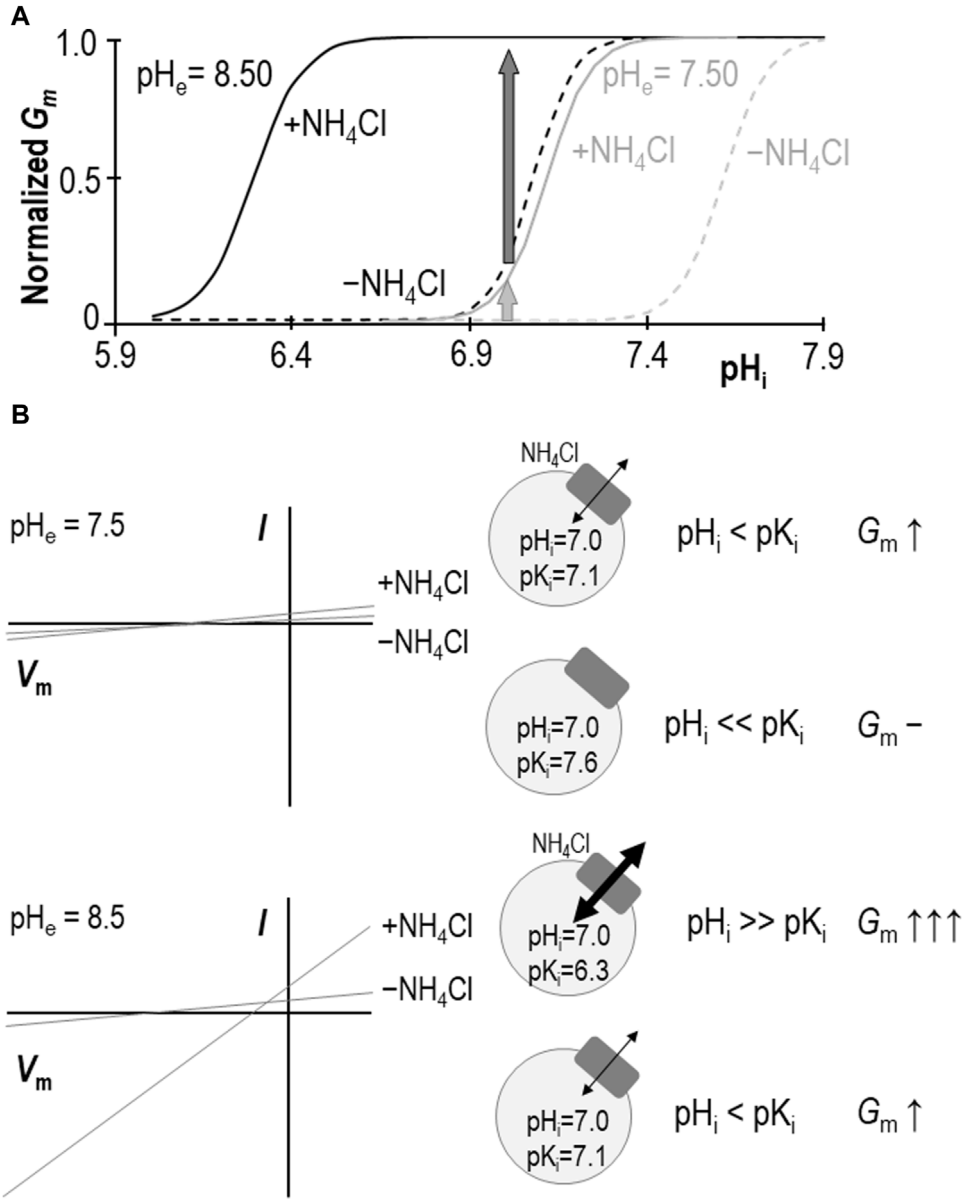

FIGURE 7
Models of SLC4A11 action in the presence and absence of NH_4Cl. **(A)** Cartoon representing the pH_i versus G_m relationships for SLC4A11 at pHe 7.50 (gray lines) and 8.50 (black lines) in the presence (solid lines) and absence (dashed lines) of 1 mM NH_4Cl. **(B)** Cartoon showing how the scheme in panel (A) could explain how NH_4Cl can achieve greater potency with respect to enhancing SLC4A11-mediated conductance at pH_e = 8.5 (lower panel) versus 7.5 (upper panel), as observed in prior studies such as Zhang et al., 2015 or Myers et al., 2016. I-V plots are cartoons, gray circles represent cells expressing SLC4A11 (gray boxes) with black arrows indicating relative magnitudes of conductance.

representative of the system and interpret them using a modified Goldman-Hodgkin-Katz equation, we can reproduce the offset by implementing a small permeability to a depolarizing cation. Two examples are provided: in Model 1, we add a sodium permeability to the system. Because the abundance of H^+ is so small compared to the abundance of Na^+, the relative permeability of Na^+ to H^+ must be very small not to completely overwhelm V_m. In this instance, $P_{Na}/P_H = 6 \times 10^{-10}$ provides a good fit to our observations. In Model 2 we add an NH_4^+ permeability to the system. We assume that $[NH_4Cl]$ is 1 mM on both sides of the membrane and calculate $[NH_4^+]_i$ for each value of pH_i. In this instance $P_{NH4}/P_H = 6 \times 10^{-8}$ provides a good fit for our data. Although the relationship curves off to an asymptote, the initial slope is Nernstian with respect to H^+, and its projection (dashed gray line) crosses the x-axis at −1.25 pH units. We note that the x-intercept of our data is also a projection and we do not know whether our data would also curve in a similar way if extended towards the x-axis. In any case this is not a critical issue as the relationship can be made to conform to the dashed line if we lower our estimate of $[NH_4Cl]_i$ to 0.1 mM. As either permeability is trivial compared to that of H^+, it does not appear to be a major confounding factor to our hypothesis. In the absence of a specific blocker, we cannot know whether the additional permeability is

10.3389/fphys.2024.1440720

$$V_m = -58 \log\left(\frac{P_H[H^+]_o + P_X[X^+]_o}{P_H[H^+]_i + P_X[X^+]_i}\right)$$

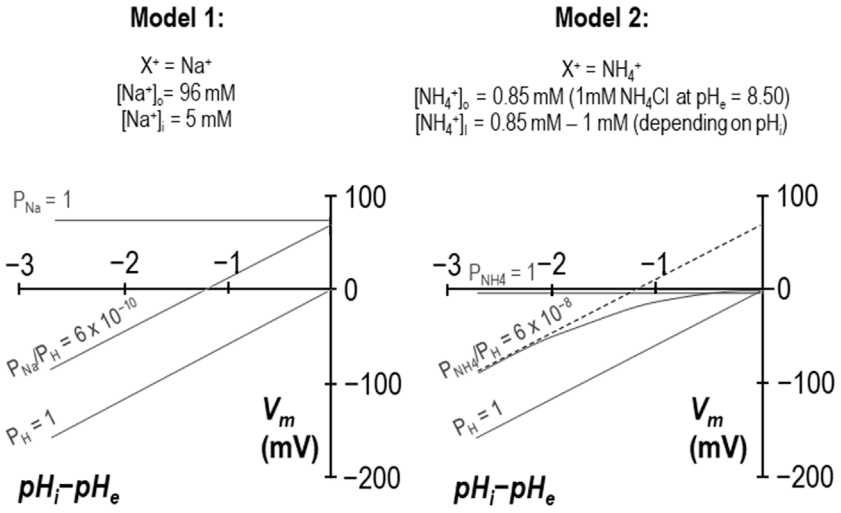

FIGURE 8
Models of additional, non-H^+ permeabilities in SLC4A11-expressing cells in the presence of NH_4Cl Two models based on a modified Goldman-Hodgkin-Katz equation in which the implementation of a small cationic permeability (either Na^+ in the case of Model 1 or NH_4^+ in the case of Model 2) causes an offset in the projected *x*-axis intercept, as observed in our experiments conducted at pH_e = 8.50 + 1 mM NH_4Cl (per Figure 4).

intrinsic to SLC4A11 or to the system in general. However, as we have only observed this in the presence of NH_4^+, and because NH_4^+ is a depolarizing influence in even H_2O-injected cells, we tentatively suggest that the *x*-axis offset represents the previously described endogenous NH_4^+ conductance.

3.4 The relationship between pK_i shifts caused by extracellular alkalinization versus NH_4Cl addition

As previously observed, in the absence of NH_4Cl, a shift of pH_e from 7.50 to 8.50, is itself sufficient to acid-shift SLC4A11 pK_i by more than 0.5 pH-units (Quade et al., 2020). If we compare SLC4A11 pK_i determined at pH_e = 7.50 + 1 mM NH_4Cl to pK_i determined at pHe = 8.50 + 0.12 mM NH_4Cl (conditions in which $[NH_3]$ is the same and pK_i is not different) we may conclude that, in the presence of NH_4Cl, pK_i has become pH_e-independent and is determined by $[NH_3]$ alone. In that case we could consider $[NH_3]$ and pH_e as activators that share a common mechanism. If SLC4A11 is less pH_e dependent in the presence of NH_4Cl, that would imply that the stimulatory effect of pH_e on SLC4A11 may have limited relevance to its *in vivo* action.

On the other hand, if we compare SLC4A11 pK_i determined at pH_e = 7.50 + 1 mM NH_4Cl to pK_i determined at pH_e = 8.50 + 1 mM NH_4Cl, values which are ~0.8 units apart, we may conclude that the phenomenon of pH_e-dependence is preserved in the presence of 1 mM NH_4Cl and that the actions of NH_4Cl and pH_e are, at least in part, mechanistically independent and additive. The common ground between these two ways of looking at the data are that the presence of NH_4Cl alters the relationship between pH_e and pK_i such that a more acidic pK_i can be achieved at a given pH_e. Interestingly, this is the opposite to a phenomenon that we have observed in relation to certain pathological SLC4A11 mutants such as R125H, in which the mutation causes pK_i to become more alkaline at a given pH_e (Quade et al., 2022). Unfortunately, the technical limitations on how far we can extend pH_i and the low resolution of our pK_i assay (due to the large standard error intrinsic to the data sets) currently preclude us from more detailed exploration of the relationship between these activating parameters.

3.5 Implications for the physiological role of SLC4A11

The fluid pumping action of corneal endothelial cells requires the action of a basolateral Na/K-ATPase to generate the transmembrane sodium gradient that drives the $Na^+/CO_3^=$ cotransporter, drawing osmolytes from the stromal fluid to discourage fluid accumulation. The pump is energized by glutaminolysis that feeds α-ketoglutarate into the TCA cycle to generate ATP; a side product of this reaction is NH_3 (Zhang et al., 2017). We have previously hypothesized that acid-loading by SLC4A11 could be useful to stabilize pH_i during robust bicarbonate pump function, responding to $Na^+/CO_3^=$ cotransporter action by sensing a local rise in pH_i (Myers et al., 2016; Nehrke, 2016). Our new data indicate that SLC4A11 is a H^+ conductor both in the presence and absence of NH_4Cl and thus that NH_3/NH_4^+ is an allosteric activator rather than a cotransported substrate of SLC4A11. This action is incompatible with a role of

corneal endothelial SLC4A11 in mediating the export of excess NH_3 from glutaminolysis, and incompatible with SLC4A11 being able to harness an outwardly-directed NH_3 gradient to mediate H^+ efflux. Because the electrochemical gradient for H^+ is typically inwardly directed, we predict that a rise in intracellular NH_3/NH_4^+ promotes H^+ influx independent of any rise in pH_i. The ability of NH_3/NH_4^+ to acid shift pK_i implies that the ability of SLC4A11 to support pump function is potentiated by NH_3/NH_4^+, the generation of which could be considered to be a proxy for the energetic requirements of the pump.

3.6 Summary

The presence of NH_4Cl causes an acidic shift in the pK_i of human SLC4A11, which translates to an increase in G_m at physiological values of pH_i. The presence of NH_4Cl does not affect the H^+ selectivity of SLC4A11, thus we conclude that NH_4Cl is an allosteric activator of SLC4A11-mediated H^+ conductance. The influence of increasing [NH_4Cl] upon SLC4A11 activity is reminiscent of the influence of increasing pH_e, but further work will be required to determine whether these share a common mechanism.

4 Materials and methods

4.1 Oocyte preparation and culture

Ovaries were harvested from female *Xenopus laevis* (*Xenopus* Express, Brooksville, FL) in accordance with the protocol approved by the University at Buffalo Institutional Animal Care and Use Committee. Frogs were anesthetized in 0.2% tricaine solution, ovariectomized, and euthanized by exsanguination. Extracted tissue was cut into ~1 cm^2 pieces and washed in a Ca^{2+}-free solution (82 mM NaCl, 2 mM KCl, 20 mM $MgCl_2$, 5 mM HEPES, pH 7.50). Oocytes were liberated by digestion in 2 mg/mL type 1A collagenase solution, and the isolated cells were washed further in the Ca^{2+}-free solution to remove the collagenase prior to resuspension in a physiological buffer (ND96: 96 mM NaCl, 2 mM KCl, 1.8 mM $CaCl_2$, 1 mM $MgCl_2$, 5 mM HEPES, pH 7.50, 200 mOsmol/kg H_2O). Until experimental use, oocytes were cultured at 18°C in OR3 medium (14 g/L Leiboviz's L-15 medium powder, 5 mM HEPES, 20 mL/L 100x penicillin-streptomycin, pH 7.50, 200 mOsmol/kg H_2O).

4.2 cRNA preparation and injection

Our starting material was a clone of human SLC4A11-B in pBSXG4 vector. The construct was linearized with HindIII, which cuts at a site downstream of the open reading frame providing a termination point for transcription. The linearized DNA was purified using a MinElute PCR Purification Kit (QIAgen, Germantown, MD) used as a template for cRNA synthesis using the T7 mMESSAGE mMACHINE kit (Invitrogen, Carlsbad, CA). cRNA was purified using an RNeasy MinElute Cleanup KIt (QIAgen). 25 ng of cRNA or H_2O was injected into each oocyte using a Nanoject programmable injector (Drummond Scientific, Broomall, PA).

4.3 Electrophysiology

Oocytes were placed into chamber (RC-3Z: Warner Instruments, Hamden, CT) on an anti-vibration table (Vision IsoStation; Newport Corp., Irvine, CA) and were superfused at 2 mL/min with solutions fed from syringe pumps (Harvard Apparatus, Holliston, MA). Borosilicate glass capillaries (BF200-156-10: Sutter Instrument, Novato, CA) were pulled into microelectrodes (such that they exhibited a tip resistance of 0.1–2 MΩ when filled with saturated KCl solution) using a micropipette puller (P-1000: Sutter Instrument). Oocytes were impaled with two such KCl-filled microelectrodes (one current-passing and one voltage-sensing) connected to an oocyte clamp (OC275: Warner Instruments, Hamden, CT). A bath clamp (725I: Warner Instruments) was used to hold the potential of the chamber fluid at 0 mV. Current-voltage (I-V) plots were gathered in 20 mV, 100 ms steps, returning to the spontaneous membrane potential for 100 ms between each step. H^+-selective microelectrodes were pulled in the same manner as voltage electrodes but the tips were filled with hydrogen ionophore I/cocktail B (Sigma Aldrich) and backfilled with a solution composed of 40 mM KH_2PO_4, 15 mM NaCl, pH 7.0. These electrodes were connected to a dual-channel electrometer (HiZ-223: Warner Instruments). Complete technical details can be found in the 2013 review by Lee, Boron, and Parker (Lee et al., 2013). Signals were digitized via a Digidata 1550 unit and captured using Clampex 10.4 software (Molecular Devices LLC, San Jose) and custom continuous acquisition software (written by Mr. Dale Huffman for Walter Boron's laboratory at Case Western Reserve University, Cleveland, OH).

4.4 Electrophysiology solutions

pH 7.50 solutions contained 96 mM NaCl, 2 mM KCl, 1.8 mM $CaCl_2$, 1 mM $MgCl_2$, 5 mM HEPES, 200 mOsmol/kg H_2O. pH 8.50 solutions had the same composition but were buffered with 5 mM Bicine in place of HEPES. NH_4Cl was added to NH_4Cl-containing solutions as a powder, and pH was readjusted as necessary.

4.5 Data analysis

Data are presented as means ± standard error of the mean. Slope conductance (G_m) was determined from the slope of a linear trendline fit to I-V data in Microsoft Excel. Normalized G_m data was plotted against pH_i (expressed as [OH^-]) and fit to the Hill equation using the solver add-in of Excel to determine the values of EC_{50} and N_{app} that would result in the minimum root square difference between the observed data and the outcome of the Hill equation:

$$\frac{G_m}{G_{m,max}} = \frac{1}{1 + \left(EC_{50}/[OH^-]\right)^{N_{app}}}$$

EC_{50} was converted into a value of pK_i using the following equation:

$$pK_i = 14 - [-log(EC_{50})]$$

For Figure 3A, we calculated $pK_{i,app}$ by solving the Hill equation for EC_{50} at each pair of G_m and $[OH^-]$ (i.e., pH_i) data points. We assumed that $G_{m,max}$ and N_{app} were constants: 79 μS and 7 respectively, corresponding to the data gathered from this cell during period "b." Calculations of $[NH_3]$ at a given pH value and $[NH_4Cl]$ assume a pK_a for the NH_3/NH_4^+ equilibrium of 9.25.

Statistical analysis was performed in Excel using unpaired t-tests, one- or two-tailed as necessary. For multiple comparison, ANOVA was performed using MiniTab software.

Data availability statement

The datasets presented in this study can be found in online repositories. The names of the repository/repositories and accession number(s) can be found below: https://doi.org/10.6084/m9.figshare.25928233.v1.

Ethics statement

The animal study was approved by IACUC at University at Buffalo Jacobs School of Medicine. The study was conducted in accordance with the local legislation and institutional requirements.

Author contributions

RP: Conceptualization, Data curation, Formal Analysis, Investigation, Methodology, Validation, Visualization, Writing–original draft, Writing–review and editing. BQ: Conceptualization, Investigation, Methodology, Visualization, Writing–review and editing. AM: Methodology, Project administration, Resources, Supervision, Writing–review and editing. MP: Conceptualization, Data curation, Formal Analysis, Funding acquisition, Investigation, Methodology, Project administration, Resources, Supervision, Validation, Visualization, Writing–original draft, Writing–review and editing.

Funding

The author(s) declare that financial support was received for the research, authorship, and/or publication of this article. This work was funded by NIH grant NEI-EY028580 to MP. RP was partially supported by an award from the Stephen Besch Scholarship fund.

Acknowledgments

Thanks to Rossana Occhipinti at Case Western Reserve University for helpful discussions and to Jacob Tondreau for technical assistance.

Conflict of interest

The authors declare that the research was conducted in the absence of any commercial or financial relationships that could be construed as a potential conflict of interest.

Publisher's note

References

Burckhardt, B. C., and Frömter, E. (1992). Pathways of NH_3/NH_4^+ permeation across *Xenopus laevis* oocyte cell membrane. *Pflugers Arch.* 420, 83–86. doi:10.1007/BF00378645

Desir, J., Moya, G., Reish, O., Van Regemorter, N., Deconinck, H., David, K. L., et al. (2007). Borate transporter SLC4A11 mutations cause both Harboyan syndrome and non-syndromic corneal endothelial dystrophy. *J. Med. Genet.* 44, 322–326. doi:10.1136/jmg.2006.046904

Frommer, W. B., and von Wirén, N. (2002). Plant biology: ping-pong with boron. *Nature* 420, 282–283. doi:10.1038/420282a

Gröger, N., Fröhlich, H., Maier, H., Olbrich, A., Kostin, S., Braun, T., et al. (2010). SLC4A11 prevents osmotic imbalance leading to corneal endothelial dystrophy, deafness, and polyuria. *J. Biol. Chem.* 285, 14467–14474. doi:10.1074/jbc.M109.094680

Han, S. B., Ang, H.-P., Poh, R., Chaurasia, S. S., Peh, G., Liu, J., et al. (2013). Mice with a targeted disruption of Slc4a11 model the progressive corneal changes of congenital hereditary endothelial dystrophy. *Invest. Ophthalmol. Vis. Sci.* 54, 6179–6189. doi:10.1167/iovs.13-12089

Hodson, S. (1977). The endothelial pump of the cornea. *Invest Ophthalmol. Vis. Sci.* 16, 589–591.

Jalimarada, S. S., Ogando, D. G., Vithana, E. N., and Bonanno, J. A. (2013). Ion transport function of SLC4A11 in corneal endothelium. *Invest. Ophthalmol. Vis. Sci.* 54, 4330–4340. doi:10.1167/iovs.13-11929

Kao, L., Azimov, R., Abuladze, N., Newman, D., and Kurtz, I. (2015). Human SLC4A11-C functions as a DIDS-stimulatable $H^+(OH^-)$ permeation pathway: partial correction of R109H mutant transport. *Am. J. Physiol. Cell Physiol.* 308, C176–C188. doi:10.1152/ajpcell.00271.2014

Kao, L., Azimov, R., Shao, X. M., Abuladze, N., Newman, D., Zhekova, H., et al. (2020). SLC4A11 function: evidence for $H^+(OH^-)$ and NH_3-H^+ transport. *Am. J. Physiol. Cell Physiol.* 318, C392–C405. doi:10.1152/ajpcell.00425.2019

Kao, L., Azimov, R., Shao, X. M., Frausto, R. F., Abuladze, N., Newman, D., et al. (2016). Multifunctional ion transport properties of human SLC4A11: comparison of the SLC4A11-B and SLC4A11-C variants. *Am. J. Physiol. Cell Physiol.* 311, C820–C830. doi:10.1152/ajpcell.00233.2016

Lee, S.-K., Boron, W. F., and Parker, M. D. (2013). Monitoring ion activities in and around cells using ion-selective liquid-membrane microelectrodes. *Sensors (Basel)* 13, 984–1003. doi:10.3390/s130100984

Lee, S.-K., Occhipinti, R., Moss, F. J., Parker, M. D., Grichtchenko, I. I., and Boron, W. F. (2022). Distinguishing among HCO_3^-, $CO_3^=$, and H^+ as substrates of proteins that appear to Be "bicarbonate". *Transp. J. Am. Soc. Nephrol. ASN* 2022030289. doi:10.1681/ASN.2022030289

Loganathan, S. K., Schneider, H.-P., Morgan, P. E., Deitmer, J. W., and Casey, J. R. (2016). Functional assessment of SLC4A11, an integral membrane protein mutated in corneal dystrophies. *Am. J. Physiol. Cell Physiol.* 311, C735–C748. doi:10.1152/ajpcell.00078.2016

Lopez, I. A., Rosenblatt, M. I., Kim, C., Galbraith, G. C., Jones, S. M., Kao, L., et al. (2009). Slc4a11 gene disruption in mice: cellular targets of sensorineuronal abnormalities. *J. Biol. Chem.* 284, 26882–26896. doi:10.1074/jbc.M109.008102

Malhotra, D., Jung, M., Fecher-Trost, C., Lovatt, M., Peh, G. S. L., Noskov, S., et al. (2020). Defective cell adhesion function of solute transporter, SLC4A11, in endothelial corneal dystrophies. *Hum. Mol. Genet.* 29, 97–116. doi:10.1093/hmg/ddz259

Musa-Aziz, R., Jiang, L., Chen, L.-M., Behar, K. L., and Boron, W. F. (2009). Concentration-dependent effects on intracellular and surface pH of exposing *Xenopus* oocytes to solutions containing NH_3/NH_4^+. *J. Membr. Biol.* 228, 15–31. doi:10.1007/s00232-009-9155-7

Myers, E. J., Marshall, A., Jennings, M. L., and Parker, M. D. (2016). Mouse Slc4a11 expressed in *Xenopus* oocytes is an ideally selective H^+/OH^- conductance pathway that is stimulated by rises in intracellular and extracellular pH. *Am. J. Physiol. Cell Physiol.* 311, C945–C959. doi:10.1152/ajpcell.00259.2016

Nehrke, K. (2016). H(OH), H(OH), H(OH): a holiday perspective. Focus on Mouse Slc4a11 expressed in *Xenopus* oocytes is an ideally selective H^+/OH^- conductance pathway that is stimulated by rises in intracellular and extracellular pH. *Am. J. Physiol. Cell Physiol.* 311, C942–C944. doi:10.1152/ajpcell.00309.2016

Ogando, D. G., Choi, M., Shyam, R., Li, S., and Bonanno, J. A. (2019). Ammonia sensitive SLC4A11 mitochondrial uncoupling reduces glutamine induced oxidative stress. *Redox Biol.* 26, 101260. doi:10.1016/j.redox.2019.101260

Ogando, D. G., Jalimarada, S. S., Zhang, W., Vithana, E. N., and Bonanno, J. A. (2013). SLC4A11 is an EIPA-sensitive Na^+ permeable pH_i regulator. *Am. J. Physiol. Cell Physiol.* 305, C716–C727. doi:10.1152/ajpcell.00056.2013

Park, M., Li, Q., Shcheynikov, N., Zeng, W., and Muallem, S. (2004). NaBC1 is a ubiquitous electrogenic Na^+-coupled borate transporter essential for cellular boron homeostasis and cell growth and proliferation. *Mol. Cell* 16, 331–341. doi:10.1016/j.molcel.2004.09.030

Parker, M. D., and Boron, W. F. (2013). The divergence, actions, roles, and relatives of sodium-coupled bicarbonate transporters. *Physiol. Rev.* 93, 803–959. doi:10.1152/physrev.00023.2012

Parker, M. D., Ourmozdi, E. P., and Tanner, M. J. (2001). Human BTR1, a new bicarbonate transporter superfamily member and human AE4 from kidney. *Biochem. Biophys. Res. Commun.* 282, 1103–1109. doi:10.1006/bbrc.2001.4692

Quade, B. N., Marshall, A., and Parker, M. D. (2020). pH dependence of the Slc4a11-mediated H^+ conductance is influenced by intracellular lysine residues and modified by disease-linked mutations. *Am. J. Physiol. Cell Physiol.* 319, C359–C370. doi:10.1152/ajpcell.00128.2020

Quade, B. N., Marshall, A., and Parker, M. D. (2022). Corneal dystrophy mutations R125H and R804H disable SLC4A11 by altering the extracellular pH dependence of the intracellular pK that governs $H^+(OH^-)$ transport. *Am. J. Physiol. Cell Physiol.* 323, C990–C1002. doi:10.1152/ajpcell.00221.2022

Vilas, G. L., Loganathan, S. K., Liu, J., Riau, A. K., Young, J. D., Mehta, J. S., et al. (2013). Transmembrane water-flux through SLC4A11: a route defective in genetic corneal diseases. *Hum. Mol. Genet.* 22, 4579–4590. doi:10.1093/hmg/ddt307

Vithana, E. N., Morgan, P., Sundaresan, P., Ebenezer, N. D., Tan, D. T. H., Mohamed, M. D., et al. (2006). Mutations in sodium-borate cotransporter SLC4A11 cause recessive congenital hereditary endothelial dystrophy (CHED2). *Nat. Genet.* 38, 755–757. doi:10.1038/ng1824

Vithana, E. N., Morgan, P. E., Ramprasad, V., Tan, D. T. H., Yong, V. H. K., Venkataraman, D., et al. (2008). SLC4A11 mutations in Fuchs endothelial corneal dystrophy. *Hum. Mol. Genet.* 17, 656–666. doi:10.1093/hmg/ddm337

Weiss, J. S., Rapuano, C. J., Seitz, B., Busin, M., Kivelä, T. T., Bouheraoua, N., et al. (2024). IC3D classification of corneal dystrophies-edition 3. *Cornea* 43, 466–527. doi:10.1097/ICO.0000000000003420

Zhang, W., Li, H., Ogando, D. G., Li, S., Feng, M., Price, F. W., et al. (2017). Glutaminolysis is essential for energy production and ion transport in human corneal endothelium. *EBioMedicine* 16, 292–301. doi:10.1016/j.ebiom.2017.01.004

Zhang, W., Ogando, D. G., Bonanno, J. A., and Obukhov, A. G. (2015). Human SLC4A11 is a novel NH_3/H^+ Co-transporter. *J. Biol. Chem.* 290, 16894–16905. doi:10.1074/jbc.M114.627455